Carbohydrate Research 346 (2011) 759–768

Contents lists available at ScienceDirect

Carbohydrate Research

journal homepage: www.elsevier.com/locate/carres

Utility of coupled-HSQC experiments in the intact structural elucidation of three complex saponins from *Blighia sapida*

Eugene P. Mazzola [a,*], Ainsley Parkinson [b], Edward J. Kennelly [b], Bruce Coxon [c], Linda S. Einbond [d], Darón I. Freedberg [e,*]

[a] University of Maryland-FDA Joint Institute, College Park, MD 20742, USA
[b] Lehman College, CUNY, Bronx, NY 10468, USA
[c] The Eunice Kennedy Shriver National Institute of Child Health and Human Development, NIH, Bethesda, MD 20892, USA
[d] Herbert Irving Comprehensive Cancer Center, College of Physicians and Surgeons of Columbia University, New York, NY 10032, USA
[e] Center for Biologics Evaluation and Research, FDA, Bethesda, MD 20852, USA

ARTICLE INFO

Article history:
Received 12 November 2010
Received in revised form 18 February 2011
Accepted 21 February 2011
Available online 25 February 2011

Keywords:
Ackee
Blighia sapida
Coupled-HSQC
Triterpene glycosides
Saponins

ABSTRACT

The structures of three complex saponins from the fruit pods of *Blighia sapida* have been elucidated and their ^{1}H and ^{13}C NMR spectra assigned employing a variety of one- and two-dimensional NMR techniques without degradative chemistry. The saponins have either four or six monosaccharide units linked to a triterpene aglycone. High-resolution, proton-coupled-HSQC spectra were important for determining both the identities of the intact monosaccharide units and coupling constants in strongly coupled proton spin systems. These NMR experiments will prove crucial as the complexity of saponin structures reaches the limit that can be determined solely by NMR.

1. Introduction

Blighia sapida König, also known as ackee, is a tropical to subtropical plant in the soapberry family (*Sapindaceae*) and indigenous to equatorial Africa. It is cultivated in the West Indies, Central and South America, and Florida for its edible yellow fruit arils. The fruit is obtuse or pear shaped, and either yellow, red, or yellow-red in color and splits open longitudinally when exposed to sunlight during the mature stage.[1] The immature, unripe ackee fruit, contains high levels of toxic cyclopropyl peptides hypoglycin A and B, which have been implicated as the cause of the 'Jamaican vomiting sickness'.[2,3] The immature fruit juice has been used as a rub to treat ringworm and skin conditions in domesticated animals.[4] The pods and seeds are employed as a fish poison, due to their saponin content, as well as in soap-making, after having been ashed.[5] Additionally, the edible fruit arils and the leaves have industrial application and medicinal properties, such as the treatment of fever and conjunctivitis.[1]

Previous chemical investigations of ackee reported the isolation of six principal groups of compounds: triterpenes, steroids, and their glycosides (collectively called saponins), sesquiterpenes, quinines, alkaloids, and polyphenols.[6–10] Recent work in one of our laboratories has resulted in the isolation of six known polyphenols, to which the high antioxidant activity and total phenolic content of the ackee pods are attributed.[11] To date, only a small number of triterpenes has been found, and these exhibited various biological activities including anti-cancer and molluscicidal activity.[12] This paper describes the isolation and structural determination of three monodesmosidic triterpenoid saponins, blighosides A (**1**), B (**2**), and C(**3**). Because the three saponins were to be subjected to subsequent pharmacological testing, *vide infra*, and were available in limited quantities, it was decided not to employ classical degradative methods that are commonly used in the structural determination of complex saponins.[13,14]

* Corresponding authors. Tel.: +1 301 405 1826; fax: +1 301 314 9121 (E.P.M.); tel.: +1 301 496 0837; fax +1 301 480 1115 (D.I.F.).
E-mail addresses: emazzola@umd.edu (E.P. Mazzola), ainsley.parkinson@lehman.cuny.edu (A. Parkinson), Edward.kennelly@lehman.cuny.edu (E.J. Kennelly), coxonb@mail.nih.gov (B. Coxon), l.einbond@gmail.com (L.S. Einbond), daron_freedberg@nih.gov (D.I. Freedberg).

0008-6215/$ - see front matter © 2011 Published by Elsevier Ltd.
doi:10.1016/j.carres.2011.02.019

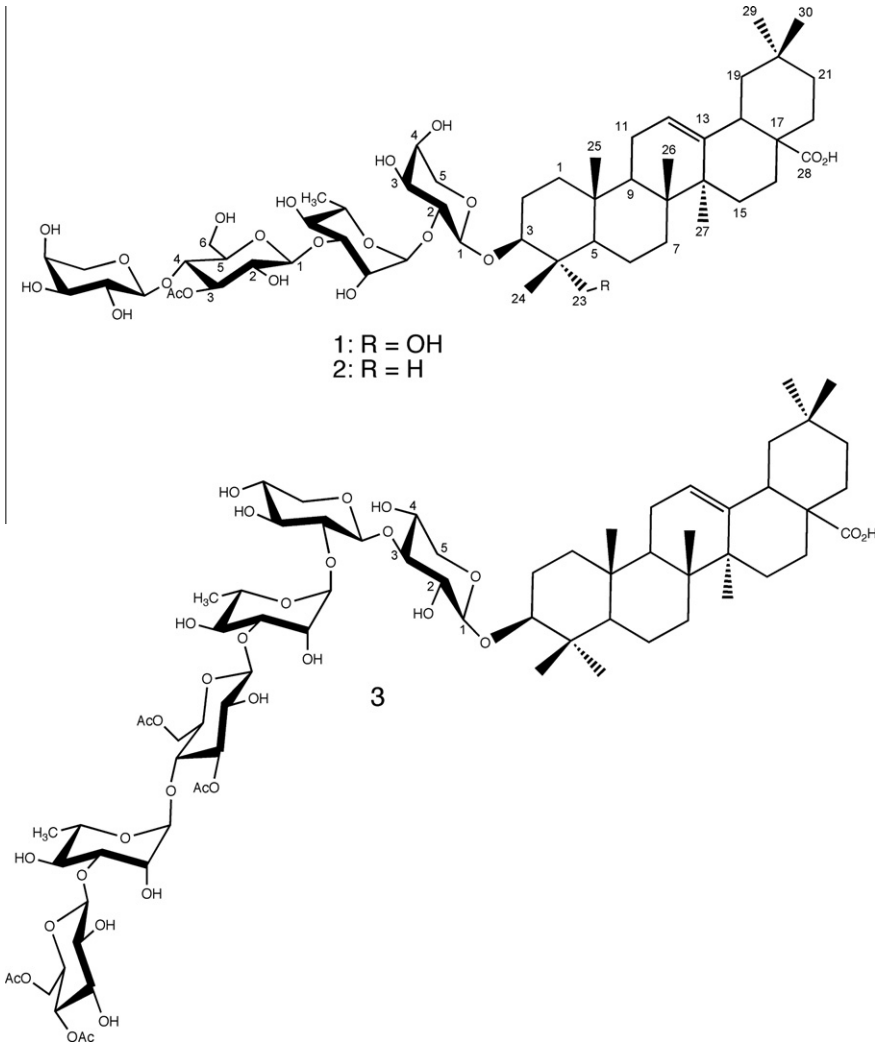

Saponins are amphipathic natural products containing an oligosaccharide linked to a mono-, di-, or triterpene, which are often used in medicinal products.[14–18] For example, digoxin consists of a triterpene aglycone core linked to a trisaccharide unit and is a well-known therapeutic agent widely used to treat heart disease. QS-21, a far more complex saponin consisting of a triterpene unit, a lipid-A like fragment and a separate branched trisaccharide, is being evaluated as an adjuvant due to its ability to boost the immune response to vaccines.[19–22] This is because either the antigens in some vaccines do not elicit a strong immune response on their own, such as in polysaccharide vaccines or because the immune systems of infants and toddlers cannot mount a strong enough immune response. Because saponins may be excipients in vaccine formulations, have extremely complex structures, and are often isolated from natural sources, it is crucial to establish methods for analysis of their structures and composition.

2. Results and discussion

2.1. Mass spectral results

The most abundant of the three isolates, blighoside A (**1**), was isolated as a white amorphous powder. Its positive-ion, ESI-TOF mass spectrum exhibited a molecular ion peak at *m/z* 1087.5689 $[M+H]^+$, corresponding to a molecular formula of $C_{54}H_{86}O_{22}$ and requiring 12 units of unsaturation.

2.1.1. Identification of the aglycone moiety of blighoside A

^1H, ^{13}C, and DEPT NMR spectra of blighoside A suggested that this compound is a saponin and confirmed the presence of four monosaccharide units. The structure and stereochemistry of the aglycone unit were determined by a combination of the three above-mentioned experiments in addition to high-resolution HSQC and HMBC NMR experiments. ^1H and ^{13}C NMR spectra indicated that the non-glycosidic portion of blighoside A contained seven methyl groups in addition to an acetate functionality in the glycosidic part. The signals of six of these methyl groups appeared as singlets in the ^1H NMR spectrum and displayed HMBC connectivities to ^{13}C signals that were in the aglycone, and not the glycosidic region of the ^{13}C NMR spectrum. Methyl hydrogens display especially strong HMBC correlations, and two- and three-bond

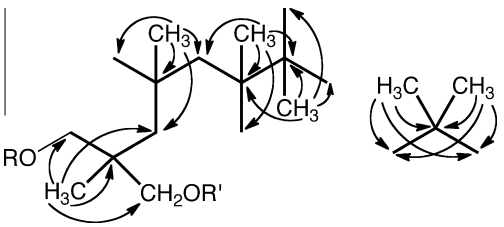

Figure 1. HMBC correlations of the six methyl groups of blighoside A (**1**).

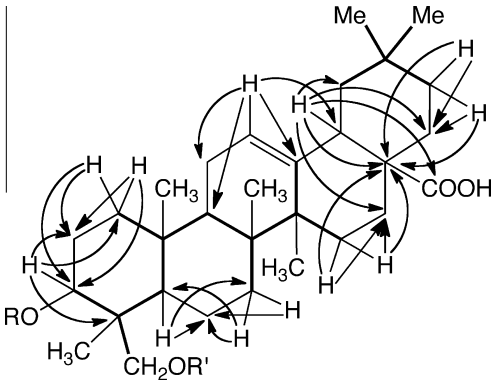

Figure 2. Important HMBC correlations of the remaining hydrogens of blighoside A (**1**).

Table 1
^{13}C and ^{1}H Chemical Shift Data of **1** [in ppm relative to $(CH_3)_4Si$ in CD_3OD]

Position	^{13}C shift (ppm)	^{1}H shift (ppm)	HMBC connectivity
1	39.82	1.61 ddd (13.2, 3.6, 3.6) eq 0.97 ddd (13.9, 13.2, 3) ax	3, 5, 25
2	26.76	1.87 dddd (13.9, 4.7, 3.6, 3) eq 1.75 dddd (13.9, 13.9, 11.8, 3.6) ax	1AB, 3
3	82.55	3.62 dd (11.8, 4.7) ax	1AB, 2AB, 5, 23AB, 24, Ara-I-1
4	44.12		2AB, 3, 23AB, 24
5	48.27	1.27 dd (11.7, 1) ax	1A, 3, 7AB, 9, 23AB, 24, 25
6	18.96	1.51 dddd (13.2, 4, 4, 1) eq 1.38 dddd (13.2, 13.2, 11.7, 3.4) ax	5, 7AB
7	33.56	1.63 ddd (13.2, 13.2, 4) ax 1.27 ddd (13.2, 4, 3.4) eq	5, 9, 26
8	40.66		6AB, 11, 26, 27
9	49.14	1.64 dd (10.6, 7.8) ax	5, 7AB, 12, 25, 26
10	37.77		2AB, 6AB, 25
11	24.67	1.91 ddd (13.8, 10.6, 3.8) ax 1.89 ddd (13.8, 7.8, 3.8) eq	9, 12
12	123.75	5.25 t (3.8)	11, 18
13	145.39		11, 15B, 18, 19AB, 27
14	43.12		12, 16AB, 18, 26, 27
15	28.99	1.78 ddd (13.8, 13.7, 4.3) ax 1.08 ddd (13.8, 4.2, 3.3) eq	16AB, 27
16	24.21	2.02 ddd (13.7, 13.6, 4.2) ax 1.60 ddd (13.6, 4.3, 3.3) eq	18, 22A
17	47.78		15AB, 19B, 21AB
18	42.88	2.85 dd (13.8, 4.5)	12, 16AB, 22AB
19	47.39	1.70 t (13.8) ax 1.13 ddd (13.8, 4.5, 2) eq	21AB, 29, 30
20	31.75		18, 22B, 29, 30
21	35.05	1.39 ddd (13.6, 13.5, 3.4) ax 1.21 dddd (13.5, 3.5, 3.4, 2) eq	19AB, 29, 30
22	33.96	1.75 ddd (13.6, 13.6, 3.5) ax 1.54 ddd (13.6, 3.4, 3.4) eq	16AB
23	64.72	3.56, 3.34 AB (11.2)	3, 5, 24
24	13.88	0.71 ax	3, 5, 23AB
25	16.55	0.98 ax	1B, 5, 9
26	17.92	0.82 ax	7A, 9
27	26.63	1.18 ax	15A
28	182.01		16A, 18, 22AB
29	33.72	0.91 eq	19A, 21A, 30
30	24.12	0.94 ax	19A, 21A, 29
Ara-I			
1	105.12	4.49 d (6.5) ax	3, Ara-I-5A
2	76.88	3.65 dd (9.7, 6.5) ax	Rha-1, Ara-I-4
3	74.20	3.66 dd (9.7, 3.8) ax	Ara-I-5A
4	70.13	3.758 ddd (3.8, 2.3, 2) eq	Ara-I-3, Ara-I-5AB
5	67.79	3.83 dd (12.6, 2.3) eq 3.53 dd (12.6, 2) ax	Ara-I-4

Table 1 (*continued*)

Position	^{13}C shift (ppm)	^{1}H shift (ppm)	HMBC connectivity
Rha-II			
1	101.78	5.23 d (1.7) eq	Ara-I-2, Rha-2
2	71.26	4.23 dd (3.2, 1.7) eq	Rha-1, Rha-3
3	83.01	3.897 dd (9.6, 3.2) ax	Glc-1, Rha-1, Rha-2
4	72.72	3.56 t (9.6) ax	Rha-2, Rha-5, Rha-6
5	70.20	3.90 dq (9.6, 6.2) ax	Rha-1, Rha-6
6	18.24	1.26 d (6.2) eq	Rha-5
Glc-III			
1	105.67	4.60 d (7.8) ax	Rha-3, Glc-2
2	73.68	3.48 dd (9.5, 7.8) ax	Glc-1, Glc-3
3	76.82	5.04 t (9.5) ax	Glc-2, Glc-4
4	77.72	3.74 t (9.5) ax	Ara-IV-1, Glc-3, Glc-5
5	76.79	3.49 ddd (9.5, 3.3, 3.1) ax	Glc-4, Glc-6AB
6	61.43	3.93 dd (12.2, 3.3), 3.895 dd (12.2, 3.1)	Glc-4, Glc-5
3-OAc	CO = 173.24 CH_3 = 21.67	CH_3 = 2.10	Glc-3, CH_3 = 2.10
Ara-IV			
1	106.03	4.20 d (6.8) ax	Glc-4, Ara-IV-5A
2	72.68	3.46 dd (9.7, 6.8) ax	Ara-IV-1, Ara-IV-4
3	74.54	3.47 dd (9.7, 3.8) ax	Ara-IV-5A
4	69.93	3.765 ddd (3.8, 3.8, 2.2) eq	Ara-IV-3, Ara-IV-5AB
5	65.88	3.84 dd (12.4, 3.8) eq 3.52 dd (12.4, 2.2) ax	Ara-IV-4

correlations from these methyl groups in addition to those from other critical hydrogens permitted structural identification of the aglycone.

The structure of this triterpene was arrived at in the following manner. Two methyl groups (C29 and C30) and a methyl and CH_2OH group (C24 and C23, respectively) were shown by the HMBC spectrum to be geminal pairs, and the six methyl groups exhibited the following connectivities: (i) CH_3-24 (δ 0.71) to 82.55 (C3), 64.72 (C23), 44.12 (C4), and 48.27 (C5) ppm, (ii) CH_3-25 (δ 0.98) to 39.82 (C1), 48.27 (C5), 49.14 (C9), and 37.77 (C10) ppm, (iii) CH_3-26 (δ 0.82) to 33.56 (C7), 40.66 (C8), 49.14 (C9), 43.12 (C14) ppm, (iv) CH_3-27 (δ 1.18) to 40.66 (C8), 145.39 (C13), 43.12 (C14), and 28.99 (C15) ppm, (v) CH_3-29 (δ 0.91)/CH_3-30 (δ0.94) to 47.39 (C19), 31.75 (C20), and 35.05 (C21) ppm. These HMBC correlations, together with HSQC and short mixing-time TOCSY connectivities, permitted the identification of 21 carbons, and the direct linking of 16 carbons, belonging to the aglycone (Fig. 1). The remaining nine carbons were identified and placed in the developing structure, together with the five-carbon fragment that includes the geminal-dimethyl group, by means of their hydrogen and carbon HMBC connectivities to portions of the structure that had been previously elucidated (Fig. 2, Table 1).

Determination of the stereochemistry at C3 and C4 and assignment, as axial or equatorial, of virtually all of the hydrogens and methyl groups of compound **1** was accomplished in several ways. For certain methine hydrogens, such as H3, observation of a large (10–12 Hz) vicinal coupling required that they be axial. Likewise, H16A was determined to be axial by virtue of the two large couplings (13.6 and 13.7 Hz) exhibited in its ^{1}H NMR spectrum. For other methine hydrogens, such as H5 and H9, whose signals are located in congested regions of the ^{1}H NMR spectrum, strong ROESY cross peaks between these hydrogens and H3 indicated that they too are axial. Similarly, strong HMBC cross peaks between H3 and H5 to CH_3-24 and weak correlations between these hydrogens and C23 dictated that CH_3-24 is axial and C23 equatorial. The assignments of CH_3-29 as equatorial and CH_3-30 as axial were

made also on the basis of strong HMBC cross peaks between the latter and H19A (δ 1.70) and H21A (δ 1.39) and weak correlations between the former and these hydrogens.

Finally, ROESY spectra were most helpful in determining the relative orientations of methylene hydrogens. In this manner, hydrogens 1B (δ 0.97), 3, 5, 7A (δ 1.63), 9, 16A (δ 2.02), 19A (δ 1.70), and 21A (δ 1.39) and CH_3-27 displayed strong ROESY cross peaks and are situated on the α-face ('bottom') of **1**. Conversely, hydrogens 2B (δ 1.75), 6B (δ 1.38), and 15A (δ 1.78) and methyls 24, 25, and 26 exhibited strong ROESY correlations and are, therefore, located on the β-face ('top') of **1**. Similarly, hydrogens 18 and 22A (δ 1.75) and CH_3-30 are situated on the β-face of the E-ring of **1**. Therefore, the aglycone is the known triterpene 3β,23-dihydroxy-Δ^{12}-oleanen-28-carboxylic acid, commonly called hederagenin, and one of the most common saponin aglycones.[14]

2.1.2. Identification of the monosaccharide units of blighoside A

Inspection of the ^{1}H, ^{13}C, and DEPT NMR spectra of blighoside A revealed the presence of four anomeric hydrogens and carbons and suggested that this compound is a tetrasaccharide. The broadened singlet observed for the hydrogen at δ 5.23 and the ca. 7 Hz doublets seen for those between 4.20 and 4.60 ppm indicated that these anomeric hydrogens are equatorial and axial, respectively, and that **1** possesses one α- and three β-linkages. In order to determine which proton signals belonged to what sugar units, TOCSY spectra were recorded with 10-ms and 100-ms mixing times. Inspection of the cross-sections of the latter, through both the anomeric hydrogens and the CH_3-hydrogens of the 6.2 Hz (non-aglycone) doublet at δ 1.26, identified those ^{1}H NMR signals associated with each anomeric hydrogen and the methyl group. Analysis of the former (COSY-like) spectra permitted the sequencing of hydrogens in each monosaccharide unit. In this way, one α-linked and one β-linked aldohexose and two β-linked aldopentoses were identified.

The next step in the overall monosaccharide identification process was to determine the relative *orientation* of the remaining, *non-anomeric*, ring hydrogens in each pyranoside sugar unit from their coupling constants and multiplicities. Two ring hydrogens, in both **1** and **2**, were ca. 10 Hz triplets in both their ^{1}H NMR and HSQC spectra and were accordingly recognized as axial hydrogens that are, in turn, flanked by axial hydrogens. However, such additional identification was essentially impossible from both types of spectra, due to severe signal overlap in the congested carbohydrate region of the ^{1}H NMR spectrum (Fig. 3) and insufficient resolution in the HSQC spectra.

An elegant but lesser used technique, the F_2-coupled-HSQC experiment, (^{13}C–^{1}H coupling is observed in the F_2-dimension where cross peaks appear as horizontal pairs) permits the orientation of carbohydrate ring hydrogens to be determined.[23] High-resolution coupled-HSQC spectra were obtained for ^{1}H and ^{13}C spectral regions that included just the carbohydrate region (see Section 3). These spectra provided the magnitude of anomeric one-bond ^{13}C–^{1}H couplings, and this information is useful in distinguishing axial from equatorial anomeric hydrogens because the one-bond ^{13}C–^{1}H couplings of the former are ca. 160 Hz while those of the latter are ca. 170 Hz.[24]

Much more importantly, high-resolution F_2-coupled-HSQC spectra (e.g., Fig. 4) also furnish the magnitude of ^{1}H–^{1}H (vicinal) couplings, that is, coupling information is obtained for ^{12}C-attached hydrogens that are adjacent to a ^{13}C-bonded hydrogen, which is detected in an HSQC experiment. This information can be critical for complex saponins due to both considerable ^{1}H NMR spectral overlap in the carbohydrate region (between 3.4 and 3.9 ppm) and the occurrence of vicinal hydrogens that have nearly identical chemical shifts. The determination of vicinal couplings, in both 1D ^{1}H NMR and 2D spectra, is greatly complicated due to the resulting strong coupling of these hydrogens.[25]

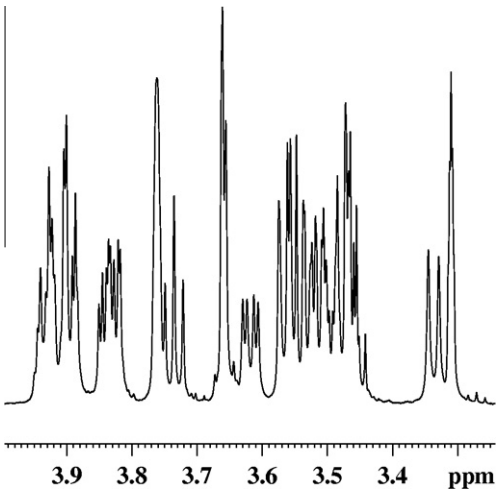

Figure 3. One-dimensional ^{1}H NMR spectrum displaying the congestion in the carbohydrate region of **1**, where most of the carbohydrate ^{1}Hs resonate.

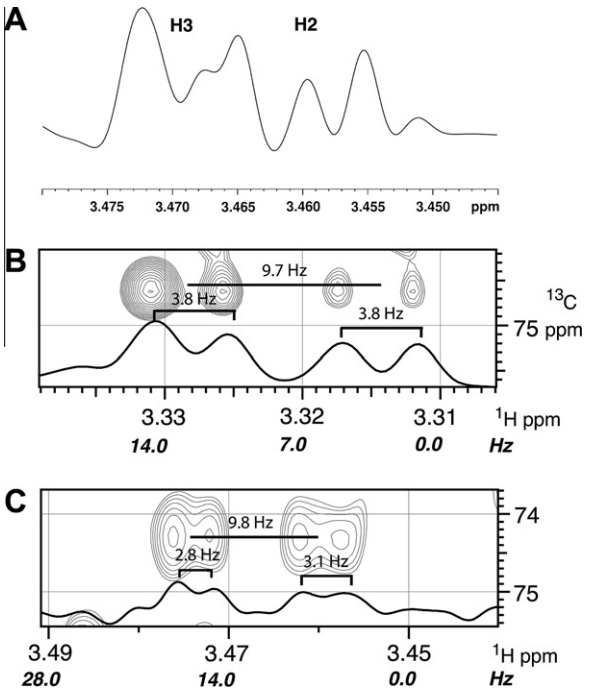

Figure 4. Various NMR spectra of the arabinose-IV region of **1**: (A) One-dimensional ^{1}H spectrum displaying the overlap of the H2 and H3 signals. (B) Right-hand (high-field) doublet component of the F_2-coupled-HSQC cross peak of H3-C3. (C) Standard decoupled HSQC cross peak of H3-C3. Note the difference in the apparent ^{1}H-^{1}H coupling constants for the smaller doublets in panel B as compared to panel C, which is due to strong ^{1}H-^{1}H coupling. Removing the carbon decoupling from the NMR experiment yields more accurate coupling constants.

However, in an F_2-coupled-HSQC spectrum, ^{1}H–^{1}H couplings are determined for subunits of the type ^{1}H–^{13}C–^{12}C–^{1}H. Here, the ca. 140 Hz, one-bond, ^{13}C–^{1}H coupling effectively results in *weak* ^{1}H–^{1}H coupling by moving the chemical shift of the ^{13}C-attached hydrogen ca. 70 Hz [J(CH)/2] away from one or two ^{12}C-bonded hydrogens. Strongly coupled, second-order spectra are thereby transformed into easily interpretable pseudo-first-order spectra.[25] This technique is analogous to the use of ^{13}C satellite signals in ^{1}H NMR spectra to determine couplings between otherwise magnetically equivalent nuclei that are normally inaccessible in typical ^{1}H NMR spectra.[26]

While the F_2-coupled-HSQC experiment greatly simplifies ^{1}H signals with significant overlap, the right-hand (high-field) and left-hand (low-field) cross peaks can differ considerably in appearance when coupled ^{1}H resonances are separated by ca. 70 Hz. In this special case, one signal of the ^{13}C-attached hydrogen will be very close, and thus strongly coupled, to the ^{12}C-attached hydrogen that is ca. 70 Hz distant. However, the other signal of the ^{13}C-attached hydrogen doublet will be ca. 140 Hz away and hence weakly coupled. It will thus appear as described above.

Information obtained from the F_2-coupled-HSQC spectra permitted identification of the four monosaccharides of blighoside A as one rhamnose, one glucose, and two arabinose units. Rhamnose was easily identified both by an equatorial anomeric hydrogen, a broad singlet at δ 5.23, and a 6.2 Hz methyl doublet at δ 1.26. As an example of (i) the type of ^{1}H–^{1}H coupling information that can be obtained from these F_2-coupled HSQC experiments and (ii) the ease with which it can be interpreted, traces for the directly bonded hydrogen–carbon pairs, H1–C1 through H5–C5, of rhamnose are shown in Figure 5. First, H4 appears as a large triplet (ca. 10 Hz) in the ^{1}H NMR spectrum, and H4–C4 is also observed as a ca. 10 Hz triplet in its F_2-coupled-HSQC trace (above the red ellipses). These couplings are very important because they require that H3, H4, and H5 be all axial. Next, H3–C3 exhibits both a large and small doublet (above the red ellipses). Because H3 was just determined to be axial, the large coupling has to be to axial H4. The small coupling must, therefore, be to H2, which has to be equatorial. H2–C2 is present as a barely discernible doublet of doublets in which the H1–H2 and H2–H3 couplings are small (2 and 3 Hz in the ^{1}H NMR spectrum), consistent with H2 being equatorial. H5–C5 appears as a multiplet (below the red ellipses) due to coupling of H5 to H4 and the 6-methyl hydrogens. Lastly, H1–C1 appears as a narrow doublet, consistent with H1 being equatorial.

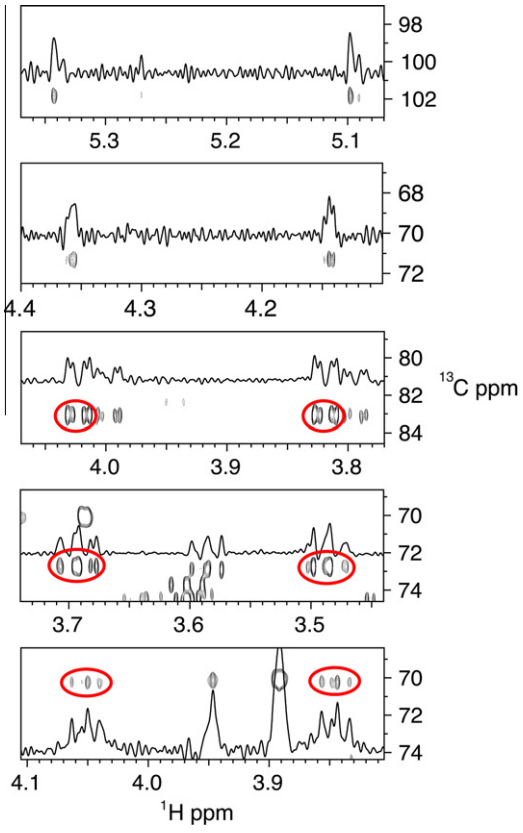

Figure 5. F_2-Coupled-HSQC traces for the directly bonded ^{1}H-^{13}C pairs H1-C1 through H5-C5, used to determine whether the ring hydrogens are axial or equatorial. These traces led us to assign the ring as that of a rhamnopyranoside.

Glucose was also readily identified because H2, H3, and H4 exhibit large, *anti*-vicinal couplings (primarily ca. 10 Hz) indicating that all are axial. The anomeric hydrogen appeared as a 7.8 Hz doublet and H5 as a broadened 9.5 Hz doublet due to coupling to H4 and the 6-methylene hydrogens; H1 and H5 are thus both axial. In addition, the considerably downfield shift of H3 (δ 5.04) suggested that the as yet unassigned acetyl group be placed at C3 of glucose. This was confirmed by the existence of an HMBC cross peak between H3 of glucose and the acetyl carbonyl carbon at δ 173.24.

The two remaining sugars were also relatively easily identified as arabinoses, the greatest difficulty being assignment of numerous close-lying signals to their proper monosaccharide unit. Fortunately, there was sufficient signal dispersion at 700 MHz to accomplish this differentiation. The arabinose anomeric hydrogens are observed as 6.5 and 6.8 Hz doublets and are thus axial. The 2- and 3-hydrogens of both arabinose units are separated by only 7 Hz and, therefore, comprise two, strongly coupled, second-order systems, vide supra. The resulting signals for these two sets of hydrogens are uninterpretable in the one-dimensional NMR spectrum, and those of Ara-IV are shown in Figure 4A. However, couplings of 9.7 and 3.8 Hz can readily be observed in the corresponding F_2-coupled-HSQC cross peak for H3–C3 of Ara-IV (Fig. 4B) and correspond to J_{23} and J_{34}, respectively.

The standard decoupled HSQC experiment yields spectra (Fig. 4C) that are similar to those of the F_2-coupled-HSQC experiment (Fig. 4B). However, the H3–C3 cross peak in the former is nowhere nearly as well defined a doublet of doublets as that in Figure 4B. In addition, the apparent ^{1}H-^{1}H coupling constants for the smaller doublets in Figure 4C are considerably smaller than those seen in Figure 4B and a consequence of strong ^{1}H–^{1}H coupling. Removing carbon decoupling from the NMR experiment yields coupling constants (Fig. 4B) that agree very well with literature values for arabinose.[27]

The same couplings for H3 were seen for Ara-I. Similarly, couplings of 9.7 and 6.5 Hz and 9.7 and 6.8 Hz were found for H2 in Ara-I and Ara-IV, respectively. The two large couplings of the 2-hydrogens require that they must be axial and have two axial neighbors. The large and small couplings (9.7 and 3.8 Hz) of the 3-hydrogens indicate that they are also axial and that the 4-hydrogens are equatorial. The 5B hydrogens (δ 3.52 and 3.53) were determined to be axial on the basis of the large ROESY cross peaks that they displayed with hydrogens 1 and 3 of both arabinose units.

The final step in the structural elucidation of blighoside A consisted of determination of the *linkage sites* both between the monosaccharide units and their attachment to the aglycone moiety. In the case of each interglycosidic link, complementary pairs of 3-bond HMBC connectivities were observed between (i) an anomeric hydrogen and the carbon of a second monosaccharide unit and (ii) the corresponding carbinol hydrogen of the second monosaccharide unit and the anomeric carbon of the first unit.

Likewise, complementary HMBC cross peaks between the anomeric hydrogen of arabinose-I (δ 4.49) and C3 of the aglycone (δ 82.55) and H3 of the aglycone (δ 3.62) and the anomeric carbon of arabinose-I (δ 105.12) established the point of attachment of the tetrasaccharide unit to the aglycone. These and other HMBC connectivities are listed in Table 1. In addition, complementary pairs of ROESY correlations were found between anomeric and carbinol hydrogens on opposite sides of the interglycosidic linkages and H3 of the aglycone. Blighoside A thus has the following structure: 3-*O*-[α-L-arabinopyranosyl-(1→4)-3-*O*-acetyl-β-D-glucopyranosyl-(1→3)-α-L-rhamnopyranosyl-(1→2)-α-L-arabinopyranosyl-(1→3)] hederagenin (**1**).

Table 2
^{13}C and ^{1}H Chemical Shift Data of **2** [in ppm relative to $(CH_3)_4Si$ in CD_3OD]

Position	^{13}C shift (ppm)	^{1}H shift (ppm)	HMBC connectivity
1	39.95	1.62 ddd (13.2, 3.6, 3.6) eq 0.99 ddd (13.9, 13.2, 3.2) ax	3, 5, 25
2	27.14	1.84 dddd (13.9, 4.5, 3.6, 3.2) eq 1.72 dddd (13.9, 13.9, 11.8, 3.6) ax	1AB, 3
3	90.63	3.13 dd (11.8, 4.5) ax	1AB, 2AB, 5, 23, 24, Ara-I-1
4	40.34		2AB, 3, 23, 24
5	57.15	0.79 dd (11.7, 1) ax	1A, 3, 7AB, 9, 23, 24, 25
6	19.42	1.56 dddd (13.2, 4, 4, 1) eq 1.42 dddd (13.2, 13.2, 11.7, 3.4) ax	5, 7AB
7	34.06	1.51 ddd (13.2, 13.2, 4) ax 1.32 ddd (13.2, 4, 3.4) eq	5, 9, 26
8	40.62		6AB, 11, 26, 27
9	49.11	1.64 dd (10.7, 7) ax	5, 7AB, 12, 25, 26
10	37.97		2AB, 6AB, 25
11	24.57	1.91 ddd (13.8, 10.7, 3.7) ax 1.89 ddd (13.8, 7, 3.7) eq	9, 12
12	123.54	5.24 t (3.7)	11, 18
13	145.40		11, 15B, 18, 19AB, 27
14	42.96		12, 16AB, 18, 26, 27
15	28.94	1.79 ddd (13.8, 13.7, 4.3) ax 1.07 ddd (13.8, 4.2, 3.4) eq	16AB, 27
16	24.17	2.00 ddd (13.7, 13.6, 4.2) ax 1.60 ddd (13.6, 4.3, 3.4) eq	18, 22A
17	47.82		15AB, 19B, 21AB
18	42.88	2.86 dd (13.8, 4.5)	12, 16AB, 22AB
19	47.41	1.69 t (13.8) ax 1.13 ddd (13.8, 4.5, 2) eq	21AB, 29, 30
20	31.67		18, 22B, 29, 30
21	35.02	1.39 ddd (13.6, 13.6, 3.4) ax 1.20 dddd (13.6, 3.5, 3.4, 2) eq	19AB, 29, 30
22	33.92	1.74 ddd (13.6, 13.6, 3.5) ax 1.54 ddd (13.6, 3.4, 3.4) eq	16AB
23	28.69	1.04 eq	3, 5, 24
24	17.14	0.86 ax	3, 5, 23
25	16.01	0.95 ax	1B, 5, 9
26	17.82	0.82 ax	7A, 9
27	26.44	1.16 ax	15A
28	182.31		16A, 18, 22AB
29	33.64	0.91 eq	30
30	24.12	0.94 ax	19A, 21A, 29
Ara-I			
1	105.45	4.48 d (5.4) ax	3, Ara-I-5A
2	76.94	3.70 dd (9.6, 5.4) ax	Rha-1, Ara-I-4
3	73.53	3.69 dd (9.6, 3.7) ax	Ara-I-5A
4	69.15	3.77 ddd (3.7, 2, 1) eq	Ara-I-3, Ara-I-5AB
5	67.69	3.83 dd (12.6, 2) eq, 3.52 dd (12.6, 1) ax	Ara-I-4
Rha-II			
1	101.79	5.15 d (1.8), eq	Ara-I-2, Rha-2
2	71.34	4.19 dd (3, 1.8) eq	Rha-1, Rha-3
3	82.85	3.86 dd (9.6, 3) ax	Glc-1, Rha-1, Rha-2
4	72.65	3.56 t (9.6) ax	Rha-2, Rha-5, Rha-6
5	70.10	3.88 dq (9.6, 6.2) ax	Rha-1, Rha-6
6	18.11	1.24 d (6.2) eq	Rha-5
Glc-III			
1	105.55	4.61 d (7.8) ax	Rha-3, Glc-2
2	73.61	3.46 dd (9.5, 7.8) ax	Glc-1, Glc-3
3	76.73	5.03 t (9.5) ax	Glc-2, Glc-4
4	77.53	3.74 t (9.5) ax	Ara-IV-1, Glc-3, Glc-5
5	76.70	3.47 ddd (9.5, 3.5, 3) ax	Glc-4, Glc-6AB
6	61.29	3.93 dd (12.2, 3.5), 3.86 dd (12.2, 3)	Glc-4, Glc-5
3-OAc	CO = 173.11 CH_3 = 21.53	CH_3 = 2.09	Glc-3, CH_3 = 2.09
Ara-IV			
1	105.92	4.20 d (6.8) ax	Glc-4, Ara-IV-5A
2	72.77	3.46 dd (9.6, 6.8) ax	Ara-IV-1, Ara-IV-4
3	74.45	3.45 dd (9.6, 3.7) ax	Ara-IV-5A
4	70.03	3.75 ddd (4.4, 3.7, 2.5) eq	Ara-IV-3, Ara-IV-5AB
5	64.83	3.84 dd (12.3, 4.4) eq, 3.50 dd (12.3, 2.5) ax	Ara-IV-4

2.2. Blighoside B

Blighoside B (**2**) was isolated as a white amorphous powder. Its positive-ion, ESI-TOF mass spectrum exhibited a molecular ion peak at *m/z* 1071.5737 $[M+H]^+$, corresponding to a molecular formula of $C_{54}H_{86}O_{21}$ and requiring 12 units of unsaturation.

^{1}H, ^{13}C, DEPT, HSQC, 100-ms mixing-time TOCSY, and ROESY NMR spectra of blighoside B demonstrated that the aglycone of **2** is fairly similar to **1**. Specifically, it contains one more methyl group than that of blighoside A and the two aglycone moieties differ slightly in the vicinity of C4. Moreover, the isolated 23-methylene hydrogens of **1** are absent and apparently replaced by a methyl group (δ_C 28.69; δ_H 1.04). The HMBC spectrum confirmed that C23 and C24 are a second methyl geminal pair in **2** and that CH_3-23 (δ 1.04)/CH_3-24 (δ 0.86) exhibited connectivities to δ_C 90.63 (C3), 40.34 (C4), and 57.15 (C5). The aglycone is thus the known triterpene 3β-hydroxy-Δ^{12}-oleanen-28-carboxylic acid, commonly called oleanolic acid, and a very common saponin aglycone.[14] The above spectra also indicated that the carbohydrate moiety of **2** is identical to that of **1**. HMBC (Table 2) and ROESY spectra demonstrated that this is the case. Blighoside B, therefore, has the following structure: 3-*O*-[α-L-arabinopyranosyl-(1→4)-3-*O*-acetyl-β-D-glucopyranosyl-(1→3)-α-L-rhamnopyranosyl-(1→2)-α-L-arabinopyranosyl-(1→3)] oleanolic acid (**2**).

Comparison of the chemical shifts of H3 and H5 in **1** versus those in **2** shows a marked deshielding effect as the equatorial 23-methyl of **2** becomes hydroxylated in **1**. This ca. 0.5 ppm shielding effect for the 23-methyl hydrogens is in accord with that reported by Stothers et al. for β-gauche equatorial methyl groups in substituted cyclohexanols.[28]

2.3. Blighoside C

Blighoside C (**3**) was isolated as a white amorphous powder. Its positive-ion FAB-MS mass spectrum exhibited a weak molecular ion peak at *m/z* 1505 $[M+H]^+$, corresponding to a molecular formula of $C_{72}H_{112}O_{33}$ and requiring 17 units of unsaturation.

^{1}H, ^{13}C, DEPT, HSQC, and HMBC NMR spectra of blighoside C suggested that this compound is a third saponin and confirmed the presence of six monosaccharide units. These spectra also demonstrated that the aglycone of **3** is identical to that of **2**. Marked shielding of H3 and H5 in **3**, relative to those of **1**, was again observed.

2.3.1. Identification of the monosaccharide units of blighoside C

Inspection of the ^{1}H, ^{13}C, and DEPT NMR spectra of blighoside C revealed the presence of six anomeric hydrogens and carbons and suggested that this compound is a hexasaccharide glycoside. The broadened singlets observed for the hydrogens at δ 5.18 and 5.19 and the ca. 5–8 Hz doublets seen for those at ca. 4.5–4.6 ppm indicated that these anomeric hydrogens are equatorial and axial, respectively, and that **3** possesses two α- and four β-linkages. Inspection of the cross-sections of 300-ms mixing time TOCSY spectra, through both the anomeric hydrogens and the CH_3-hydrogens of the 6.2 Hz (non-aglycone) doublets at δ 1.23, identified those ^{1}H NMR signals associated with each anomeric hydrogen and the methyl group. Analysis of COSY spectra permitted the

Table 3
^{13}C and ^{1}H Chemical Shift Data of **3** [in ppm relative to $(CH_3)_4Si$ in CD_3OD]

Position	^{13}C shift (ppm)	^{1}H shift (ppm)	HMBC connectivity
1	39.94	1.63 ddd (13.8, 4.2, 3) eq 1.01 ddd (13.8, 13.8, 3) ax	2AB, 3, 5, 9, 25
2	27.14	1.84 dddd (13.8, 3, 3, 2.7) eq 1.72 dddd (13.8, 13.8, 11.2, 4.2) ax	1AB, 3
3	90.62	3.12 dd (11.2, 2.7) ax	1A, 2AB, 5, 23, 24, Xyl-I-1
4	40.34		2AB, 3, 5, 23, 24
5	57.13	0.82 dd (11.7, 2) ax	1A, 3, 6A, 7AB, 9, 23, 24, 25
6	19.41	1.56 dddd (13.7, 2.5, 2.5, 2) eq 1.39 dddd (13.7, 13.7, 11.7, 2.5) ax	5, 7AB
7	34.06	1.51 ddd (13.7, 13.7, 2.5) ax 1.31 ddd (13.7, 2.5, 2.5) eq	5, 6B, 9, 26
8	40.61		6B, 9, 11, 26, 27
9	49.09	1.59 dd (10.6, 7) ax	7B, 11, 12, 25, 26
10	37.96		1B, 2A, 5, 6B, 9, 11, 25
11	24.56	1.90 ddd (13.8, 10.6, 3.5) ax 1.88 ddd (13.8, 7, 3.5) eq	9, 12
12	123.65	5.24 t (3.5)	11, 18
13	145.24		11, 12, 15B, 18, 19AB, 27
14	42.93		12,15A,16B,18,26,27
15	28.88	1.77 ddd (13.6, 13.6, 3.7) ax 1.09 ddd (13.6, 3.7, 3.7) eq	16AB, 27
16	24.10	2.01 ddd (13.6, 13.6, 3.7) ax 1.59 ddd (13.6, 3.7, 3.7) eq	18, 22AB
17	47.68		16A, 18, 19B, 21AB, 22AB
18	42.78	2.85 dd (13.6, 4)	12, 16AB, 19A, 22B
19	47.29	1.69 t (13.6) ax 1.11 ddd (13.6, 4, 1.8) eq	18, 21B, 29, 30
20	31.66		18, 22B, 29, 30
21	34.94	1.39 ddd (13.7, 13.7, 4) ax 1.19 dddd (13.7, 4, 4, 1.8) eq	19B, 29, 30
22	33.86	1.74 ddd (13.7, 13.7, 4) ax 1.53 ddd (13.7, 4, 4) eq	16AB, 21AB
23	28.73	1.03d (3) eq	3, 5, 24
24	17.21	0.85d (3) ax	3, 5, 23
25	16.03	0.95 ax	1B, 5, 9
26	17.76	0.81 ax	7A, 9
27	26.44	1.16 ax	15A
28	181.94		16AB, 18, 22AB
29	33.62	0.91 eq	30
30	24.02	0.94 ax	19A, 21A, 29
Xyl-I			
1	105.34	4.48 d (5.3) ax	3, Xyl-I-2, Xyl-I-5A
2	76.44	3.75 dd (7, 5.3) ax	Xyl-I-1, Xyl-I-3
3	73.57	3.69 t (7) ax	Xyl-I-2, Xyl-I-4, Xyl-I-5A, Xyl-II-1
4	69.04	3.76 ddd (7, 7, 2) ax	Xyl-I-3, Xyl-I-5AB
5	64.76	3.84 dd (9.7, 2) eq, 3.48 dd (9.7, 7) ax	Xyl-I-4
Xyl-II			
1	105.39	4.47 d (5.3) ax	Xyl-II-2, Xyl-II-5A
2	76.38	3.76 dd (7, 5.3) ax	Rha-III-1, Xyl-II-1, Xyl-II-3
3	73.69	3.70 t (7) ax	Xyl-II-2, Xyl-II-4, Xyl-II-5A
4	69.12	3.77 ddd (7, 7, 2) ax	Xyl-II-3, Xyl-II-5AB,
5	64.65	3.84 dd (9.7, 2) eq 3.47 dd (9.7, 7) ax	Xyl-II-4
Rha-III			
1	101.49	5.19 d (1.4) eq	Xyl-II-2, Rha-III-2
2	71.48	4.129 dd (3, 1.4) eq	Rha-III-1, Rha-III-3
3	82.78	3.85 dd (9.5, 3) ax	Glc-IV-1, Rha-III-1, Rha-III-2, Rha-III-4
4	72.61	3.55 t (9.5) ax	Rha-III-2, Rha-III-5, Rha-III-6
5	69.97	3.90 dq (9.5, 6.2) ax	Rha-III-1, Rha-III-6
6	18.08	1.232 d (6.2) eq	Rha-III-5
Glc-IV			
1	105.49	4.59 d (7.8) ax	Rha-V-1, Glc-IV-2
2	73.51	3.44 dd (9.4, 7.8) ax	Glc-IV-1, Glc-IV-3
3	78.41	4.95 t (9.4) ax	Glc-IV-2, Glc-IV-4
4	69.91	3.45 dd (9.8, 9.4) ax	Glc-IV-3, Glc-IV-5, Rha-V-1
5	75.17	3.59 ddd (9.8, 2.2, 1) ax	Glc-IV-4, Glc-IV-6AB
6	64.40	4.41 dd (12.2, 2.2) 4.22 dd (12.2, 1)	Glc-IV-5
3-OAc	CO = 172.5		Glc-IV-3, CH_3 = 2.11
	CH_3 = 21.11	CH_3 = 2.11	
6-OAc	CO = 172.7		Glc-IV-6B, CH_3 = 2.08
	CH_3 = 20.91	CH_3 = 2.08	
Rha-V			
1	101.54	5.18 d (1.4) eq	Glc-IV-4, Rha-V-2
2	71.51	4.13 dd (3, 1.4) eq	Rha-V-1, Rha-V-3
3	82.86	3.84 dd (9.5, 3) ax	Glc-VI-1, Rha-V-1, Rha-V-2, Rha-V-5
4	72.61	3.57 t (9.5) ax	Rha-V-2, Rha-V-2, Rha-V-6
5	69.98	3.89 dq (9.5, 6.2) ax	Rha-V-1, Rha-V-6
6	18.08	1.234 d (6.2) eq	Rha-V-5
Glc-VI			
1	105.80	4.56 d (7.8) ax	Rha-V-3, Glc-VI-2
2	75.30	3.39 dd (9.0, 7.8) ax	Glc-VI-1, Glc-VI-3
3	75.30	3.58 dd (9.7, 9.0) ax	Glc-VI-2, Glc-VI-4
4	72.19	4.81 t (9.7) ax	Glc-VI-3, Glc-VI-5
5	73.17	3.67 ddd (9.7, 2.6, 1.7) ax	Glc-VI-4, Glc-VI-6AB
6	63.77	4.21 dd (12.2, 1.7) 4.09 dd (12.2, 2.6)	Glc-VI-5
4-OAc	CO = 171.9		Glc-VI-4, CH3 = 2.08
	CH3 = 20.94	CH3 = 2.08	
6-OAc	CO = 172.5		Glc-VI-6A, CH3 = 2.08
	CH3 = 20.91	CH3 = 2.06	

sequencing of hydrogens in each monosaccharide unit. The COSY and TOCSY spectra together with one-bond $^{13}C1$–H1 couplings [ca. 172 Hz (two) and ca. 161 Hz (four)], indicated that **3** has two α-linked and two β-linked aldohexoses and two β-linked aldopentoses.

As with blighoside A, high-resolution coupled-HSQC spectra permitted the orientation of the glycosidic ring hydrogens to be determined.[23] Like **1**, two glucose and two rhamnose units were readily identified. In addition, the considerably deshielded chemical shifts of hydrogens 3 (δ 4.95), 6A (δ 4.41), and 6B (δ 4.22) in one glucose and hydrogens 4 (δ 4.81), 6A (δ 4.21), and 6B (δ 4.09) in the other indicated that the four unassigned acetyl groups be placed at the 3,6- and 4,6-positions of the two glucose units.

The two remaining sugars were also relatively easily identified as xyloses. Their anomeric hydrogens are observed as ca. 5.3 Hz doublets and are thus axial. Because the 2-hydrogens exhibit two large doublets (5.3 and 7 Hz), they must also be axial and have two axial neighbors. The 3-hydrogens appear as 7 Hz triplets and must likewise have flanking axial neighboring hydrogens. The 4-hydrogens are seen as triple doublets (7, 7, and 2 Hz) confirming that each has two axial neighbors. The 5B hydrogens (δ 3.47 and 3.48) were determined to be axial on the basis of the strong ROESY cross peaks that they displayed with hydrogens 1 and 3 of both xylose units.

The final step in the structural elucidation of blighoside C consisted, likewise, of determining the linkage sites between the monosaccharide units and their attachment to the aglycone moiety. As was the case with **1**, complementary pairs of 3-bond HMBC

connectivities were observed, for each interglycosidic link, between (i) an anomeric hydrogen and the carbon of a second monosaccharide unit and (ii) the corresponding carbinol hydrogen of the second monosaccharide unit and the anomeric carbon of the first unit. Likewise, complementary HMBC cross peaks between the anomeric hydrogen of xylose-I (δ 4.48) and C-3 of the aglycone (δ 90.62) and H3 of the aglycone (δ 3.12) and the anomeric carbon of xylose-I (δ 105.34) established the point of attachment of the hexasaccharide unit to the aglycone. These and other HMBC connectivities are listed in Table 3. In addition, complementary pairs of ROESY correlations were found between anomeric and carbinol hydrogens on opposite sides of the interglycosidic linkages and H3 of the aglycone. Blighoside C thus has the following structure: 3-*O*-[4,6-di-*O*-acetyl-β-D-glucopyranosyl-(1→3)-α-L-rhamnopyranosyl-(1→4)-3,6-di-*O*-acetyl-β-D-glucopyranosyl-(1→3)-α-L-rhamnopyranosyl-(1→2)-β-D-xylopyranosyl-(1→3)-β-D-xylopyranosyl-(1→3)] oleanolic acid (**3**). The structural elucidation of intact blighosides, entirely by NMR methods without resorting to degradative techniques commonly used in studying complex saponins,[13,14] illustrates the ability of modern NMR techniques to determine structures of considerable complexity.

2.4. Cytotoxicity

The EtOAc and *n*-BuOH partitioned fractions, saponins **1**–**3**, were evaluated for their ability to inhibit the proliferation of ER$^-$ MDA-MB-453 (Her2 overexpressing) human breast cancer cells. Based on the results, any possible structure-activity relationships among the isolated saponins were determined. Both the EtOAc and *n*-BuOH partitioned fractions demonstrated growth-inhibitory effects on the MDA-MB-453 cell line at IC_{50} = 43 μg/mL and 20 μg/mL, respectively. The isolated triterpenoid saponins, **1-3** obtained from the EtOAc fraction, and hederagenin (the aglycone of **1**) exhibited growth-inhibitory effects at IC_{50} = 10.3, 6.9, 10.0, and 69 μM, respectively, as compared to actein (12.6 μM), a triterpene glycoside isolated from the herb, black cohosh.

Blighosides A-C (**1–3**) have oleanane aglycones; **1** possesses a hederagenin sapogenin, while saponins **2** and **3** have oleanolic acid sapogenins. The three saponins exhibited growth-inhibitory activity on MDA-MB-453 cells that was comparable to that of the cycloartane-type saponin, actein. Further experiments are required to determine their relative activities. It will be especially important to compare the activity of saponins **1** and **2**, because **2** possesses a methyl group at C23 while **1** has a –CH_2OH group at that position.

According to studies involving saponins, biological activity depends on the type of aglycone, number of sugars, and the pattern and attachment of sugar units to the aglycone.[14] To examine the effect of the number of sugar units, it will be of interest to compare the tetrasaccharide saponin, **2**, and the hexasaccharide saponin, **3**, which possess identical aglycones. In addition to their cytotoxic activity against MDA-MB-453 human breast cancer cells, blighosides A and B may exhibit additional growth-inhibitory effects against other cell lines due to their structural signature, comprising a free carboxylic acid group at C28 of an oleanane-type aglycone and an α-L-rhamnopyranosyl-(1→2)-α-L-arabinopyranosyl sugar sequence at the 3-position of the aglycone, with oleanolic acid derivatives expected to be more potent than those of hederagenin sapogenins.[29,30]

3. Experimental

3.1. General experimental procedures

Melting points were determined with a Mel-Temp II melting point apparatus and are uncorrected.

Mass spectra for blighosides A and B were obtained by electrospray ionization on an Agilent G6520A high-resolution Q-TOF mass spectrometer that was connected to an Agilent 1200 capillary HPLC. Samples were dissolved in MeOH/water (9:1 v/v) with 0.1% HCOOH + 5 μm HCO_2NH_4 and directly injected at a flow rate of 200 μL/min. The capillary voltage was 3500 V. and the capillary gas temperature 300 °C. Mass measurements were made to a precision of <5 ppm.

FAB Mass spectra for blighoside C were obtained on a JEOL Sx102a double-focusing, magnetic sector instrument employing a CsI 'magic-bullet' matrix. GC analysis was carried out with a Hewlett-Packard GC (6890): column, Alltech 1-Chirasil-val, 0.25 mm × 30 m × 0.5 mm; column temp, 50-230 °C, 15 °C/min, then 230 °C for 18 min; carrier gas, N_2 and detector temperature, 270 °C. TLC analyses were performed by using Silica Gel 60 F_{254} plates with compounds visualized by spraying with a vanillin solution (1 g vanillin in 10% concd H_2SO_4 ethanolic soln). Sephadex LH-20 (25-100 μm, Pharmacia Fine Chemicals), C_{18} reversed-phase silica gel (40 μm, J. T. Baker), and Dianon HP-20 (Supelco) were used for column chromatography.

3.2. Plant material

B. sapida fruits were collected at the Fruit and Spice Park (Homestead, Florida) and transported frozen to New York City by overnight carrier. *B. sapida* fruits were weighed, cataloged, and frozen at −20 °C until analyzed.

3.2.1. Extraction and isolation

Ackee pods (11.0 kg) were homogenized with MeOH and extracted exhaustively at room temperature. The combined MeOH extract was filtered and concentrated under reduced pressure. The resulting aqueous-methanolic crude extract was partitioned three times with EtOAc. The EtOAc fractions (120 g) were combined and dried under reduced pressure. The EtOAc residue (15 g) was redissolved in MeOH–H_2O (1:4 v/v) under sonication, filtered, and separated over Si gel (600 g) placed in a sintered glass column and fractionated under vacuum (vacuum liquid chromatography, vlc), by eluting with a discontinuous gradient of $CHCl_3$–MeOH from 100% $CHCl_3$ to 100% MeOH. Fraction 6:1vlc ($CHCl_3$–MeOH, 6:1 v/v) (0.77 g) was chromatographed over C_{18} silica gel (20 g) by eluting with gradients of MeCN–H_2O, from 9:1 to 100:0, to give 30 subfractions. Fraction 21 (70 mg) afforded 19 mg of **1**, and fraction 24 (50.2 mg) yielded 4.7 mg of **2**. Fraction 8:1vlc ($CHCl_3$–MeOH, 8:1 v/v) (0.54 g) was chromatographed over RP-18 (20 g) by eluting with gradients of MeCN–H_2O, from 9:1 to 100:0, to give 22 subfractions. Subfractions 7–10 (25 mg) was further separated over LH-20 using a MeOH–H_2O (8:2 v/v) system to give 10 subfractions. Subfractions 3 and 4 were combined and purified over LH-20 eluting with MeOH–H_2O (8:2 v/v) to produce 8.9 mg of **3**.

3.3. Cell culture and cell proliferation assay

MDA-MB-453 (ER negative, Her2 over-expressing) human breast cancers were obtained from the ATCC (Manassas, VA). Cells were grown in Dulbecco's Modified Eagle's medium (DMEM) containing 10% (v/v) fetal bovine serum (FBS) at 37 °C and 5% CO_2 (Gibco BRL Life Technologies, Inc, Rockville, MD).

Cell proliferation was determined using the MTT [3-(4,5-dimethyl-2-thiazol)-diphenyl-2*H* tetrazolium bromide] (Dojindo, Tokyo, Japan) cell proliferation assay system, according to the manufacturer's instructions (Roche Diagnostic). Cells were seeded into 96-well plates at a density of 10^4 cells and allowed to attach for 24 h. The medium was then replaced with fresh medium containing the indicated test compounds at a range of concentrations

in DMSO (Sigma–Aldrich). The cells were treated for 4 days, after which they were incubated with MTT reagents and the absorbance read at 600 nm as previously described.[31] Actein standard for this assay was obtained from ChromaDex (Laguna Hills, CA). Cell viability was calculated by comparing cell counts in treated samples relative to cell counts in the untreated group.

3.4. Acid hydrolysis

Solutions of compounds (**1**–**3**) (2 mg each), consisting of 1 N HCl–MeOH (1:4 v/v, 5 mL, were placed in an incubator at 50 °C for 2 days. The solutions were then diluted with 10 mL HPLC grade water and neutralized with a 10% $NaHCO_3$ solution. The mixture was then partitioned between EtOAc and water. The EtOAc layer and the aqueous layers were dried under reduced pressure. The EtOAc residues were analyzed by TLC using a solvent system of 8:1 $CHCl_3$–MeOH that revealed the presence of hederagenin (3β,23-dihydroxy-Δ^{12}-oleanen-28-carboxylic acid) for compound **1**, as compared with authentic standards.

3.5. NMR methods

NMR spectra of blighoside A at 700 MHz were acquired at 298 K by means of a Bruker Avance-II-700 NMR spectrometer equipped with a 5 mm QXI HCNP probe equipped with shielded *xyz*-gradient coils. Data processing was performed using NMRPipe.[32] A solution of 19 mg of blighoside A in 0.3 mL of methanol-d_4 was prepared in a small test tube and the resulting solution transferred to a Shigemi NMR microcell whose glass was susceptibility matched to methanol. The residual ^{1}H of the methyl resonance was used as an internal chemical shift reference (δ = 3.31 ppm) for ^{1}H and δ = 49.1 ppm in the ^{13}C NMR spectra. ^{1}H NMR spectra were acquired using a spectral width of 5.22 ppm, 16,384-point data sets, a 70° pulse (8 μs), and a pulse recycle time of 2.5 s. No weighting or resolution enhancement was used for this 1D ^{1}H spectrum.

^{13}C NMR spectra were acquired by using 65,536 point data sets, a 70° pulse (10 μs), and a pulse recycle time of 2.5 s. Exponential multiplication with a line broadening of 1 Hz and an automatic baseline correction were used.

2D ROESY[34] and TOCSY[33] spectra, using a DIPSI-2 mixing sequence,[35] were used to confirm ^{1}H assignments. Two TOCSY experiments were run: one with a 10-ms mixing time, and the other a 100-ms mixing time. These spectra were taken with the carrier set to 2.88 ppm, a spectral window of 5.22 ppm, the initial increment in the indirect dimension set to one-half the dwell-time (increment) in this dimension, 8192 (t_2) × 512 (t_1) point data sets, zero-filled and processed to 16,384 (F_2) × 1024 (F_1) points. HSQC and HMBC spectra were used to correlate the hydrogens to their respective or nearby carbons. In addition, coupled HSQC spectra were taken to help assign the types of carbohydrate residues attached to the aglycone. HSQC and coupled HSQC NMR spectra were obtained by setting the carriers to 2.883 ppm and 100.4 ppm in ^{1}H and ^{13}C dimensions, respectively, and spectral windows to 5.22 ppm and 90 ppm, respectively, as well as 8192 (t_2) × 512 (t_1) point data sets; quadrature detection in the ^{13}C dimension was obtained using gradients for coherence selection. The coupled HSQC data reported in this paper were measured by removing the composite-pulse decoupling during FID detection. HMBC spectra were acquired with the carrier set to 4.77 ppm in ^{1}H and 69.6 ppm in ^{13}C, spectral windows of 6.0 ppm in ^{1}H, and 120 ppm in ^{13}C. These spectra were acquired in magnitude mode. The raw FIDs were zero-filled and transformed to 1024 (F_2) × 512 (F_1) points.

Values of $^1J_{C\text{-}1,H\text{-}1}$ were measured from ^{1}H-coupled 2D HSQC spectra obtained from 2048 (t_2) × 512 (t_1) point data sets. The CH coupling constants were extracted from F_2 slices of the coupled HSQC spectra. Squared sine-bell window functions shifted by π/2 rad were used in both dimensions for most of the 2D experiments, except that no shift was used for 2D COSY-30 data, and a π/4 rad shift was used for coupled 2D HSQC and HMBC. The COSY and HMBC spectra were displayed in absolute value mode. All other 2D spectra were acquired in the phase-sensitive, echo/anti-echo mode.

A solution of 4.7 mg of blighoside B in 0.3 mL of methanol-d_4 was prepared in a small test tube and the resulting solution transferred to a Shigemi NMR microcell whose glass was susceptibility matched to methanol. ^{1}H, ^{13}C, DEPT, HSQC, 100-ms mixing-time TOCSY, and ROESY NMR data were acquired and processed using the same experimental conditions as those described for blighoside A

NMR spectra of blighoside C at 500 MHz were acquired at 300 K by means of a Bruker DRX-500 NMR spectrometer equipped with a 5 mm TXI HCN cryoprobe with *z*-gradient coil. Data acquisition and processing were performed using Bruker TopSpin software version 1.3.4, running under Windows XP Pro SP2 on a HP xw4200 PC workstation. A solution of 8.9 mg of blighoside C in 0.4 mL of methanol-d_4 was used, including tetramethylsilane as an internal chemical shift reference (δ = 0) for ^{1}H and ^{13}C NMR spectra. ^{1}H NMR spectra were acquired using a spectral width of 4.01 kHz, 65,536 point data sets, a 30° pulse (2.4 μs), and a pulse recycle time of 8.2 s. The resolution of the ^{1}H spectra was enhanced by Gaussian multiplication of the FID, using a line-narrowing of –0.5 to –0.75 Hz, and a Gaussian truncation fraction of 0.3.

^{13}C NMR spectra were acquired by using 65,536 point data sets, a 45° pulse (6.7 μs), and a pulse recycle time of 2 s. Digital resolution was enhanced by forward linear prediction to 65,536 points. ^{13}C spectral editing was performed by acquisition of DEPT spectra, using ^{1}H read pulses of 45°, 90°, and 135°, but no linear prediction. Separate CH, CH_2, and CH_3 subspectra were generated from suitable combinations of the three DEPT spectra.

All 2D NMR spectra were acquired by pulsed field gradient-selected methods. 2D COSY, TOCSY, ROESY, and TOCSY-less ROESY (T-ROESY) were used to confirm ^{1}H assignments. 2D HSQC, HMBC, and 1D DEPT were used to assign ^{13}C spectra. 2D COSY, ROESY, T-ROESY, and HMBC NMR spectra were obtained by using 2048 (t_2) × 512 (t_1) point data sets, zero-filled and transformed to 2048 (F_2) × 2048 (F_1) points (COSY, ROESY, and T-ROESY) or 8192 (F_2) × 4096 (F_1) points (HMBC), whereas 2D HSQC spectra were taken from 2048 (t_2) × 512 (t_1) point data sets, linearly predicted and transformed to 8192 (F_2) × 2048 (F_1) points. Spectral processing with linear prediction was performed in the Topspin program by using the forward complex mode, with 128 coefficients and the final data sizes stated in the descriptions of the individual experiments. For 2D COSY, the read pulse was 30° (2.4 μs). 2D TOCSY data were recorded using an isotropic mixing time of 300 ms, and 16,384 (t_2) × 512 (t_1) point data sets, zero-filled and processed to 16,384 (F_2) × 2048 (F_1) points. Three 2D ROESY spectra were acquired, using spin-lock pulse times of 100, 250, and 500 ms, and for three 2D T-ROESY spectra, spin-lock times of 250, 500, and 1000 ms were used. 2D HSQC and HMBC were acquired with ^{1}H and ^{13}C spectral widths of 4.01 kHz (F_2) and 25.1 kHz (F_1), respectively.

Values of $^1J_{C\text{-}1,H\text{-}1}$ were measured from ^{1}H-coupled 2D HSQC spectra obtained from 2048 (t_2) × 512 (t_1) point data sets, linearly predicted as previously described and transformed to 8192 (F_2) × 2048 (F_1) points. The CH coupling constants were extracted from F_2 slices of the coupled HSQC spectra. Sine-bell squared window functions shifted by π/2 rad were used in both dimensions for most of the 2D experiments, except that no shift was used for 2D COSY-30 data, and a π/4 rad shift was used for coupled HSQC. 2D COSY and HMBC spectra were displayed in magnitude mode. All other 2D spectra were acquired in the phase-sensitive, echo/anti-echo mode.

Acknowledgments

The authors would like to thank Dr. Clifford E. Soll, Hunter College of the City of New York, and Dr. Noel Whittaker, University of Maryland, for mass spectral measurements.

Supplementary data

Supplementary data associated with this article can be found, in the online version, at doi:10.1016/j.carres.2011.02.019.

References

1. Morton, J. F. *Fruits of Warm Climates*; J.F. Morton: Miami, Fl., 1987. pp 269–271.
2. Addae, J. I.; Melville, G. N. W. *Indian Med. J.* **1988**, *37*, 6–8.
3. Bressler, R.; Corredor, C.; Brendel, K. *Pharmacol. Rev.* **1969**, *21*, 105–130.
4. Rashford, J. *Econ. Bot.* **2001**, *55*, 190–211.
5. Omobuwajo, T. O.; Sanni, L. A.; Olajide, J. O. *J. Food Eng.* **2000**, *45*, 43–48.
6. Asprey, G. F.; Thornton, W. W. *Indian Med. J.* **1955**, *4*, 145–168.
7. Balogun, A. A.; Fetuga, B. L. *Food Chem.* **1988**, *30*, 37–43.
8. Garg, H. S.; Mitra, C. R. *Planta Med.* **1967**, *15*, 74–80.
9. Hayes, L. J.; Plimmer, J. R.; Sue-Ho, W. M. *J. Chem. Soc.* **1963**, *15*, 744–745.
10. Stuart, K. L.; Roberts, E. V.; Whittle, Y. G. *Phytochemistry* **1975**, *15*, 332–333.
11. Parkinson, A., Ph.D. Thesis, *Phytochemical Analysis of Ackee*, City University of New York, 2007.
12. Kela, S. L.; Ogunsusi, R. A.; Ogbogu, V. C.; Nwude, N. *Rev. Elev. Med. Vet. Pays. Trop.* **1989**, *42*, 189–192.
13. Agrawal, P. K.; Jain, D. C.; Pathak, A. K. *Magn. Reson. Chem.* **1995**, *33*, 923–953.
14. Hostettmann, K.; Marston, A. *Saponins*; Cambridge University Press: Cambridge, 1995; Chapter 2 and 4.
15. Adams, M. M.; Damani, P.; Perl, N. R.; Won, A.; Hong, F.; Livingston, P. O.; Ragupathi, G.; Gin, D. Y. *J. Am. Chem. Soc.* **2010**, *132*, 1939–1945.
16. Hostettmann, K.; Lea, P. J. In *Biologically Active Natural Products*; Clarendon Press: Oxford, 1987; Vol. 27,
17. Kinghorn, A. D.; Balandrin, M. F. *Human Medicinal Agents from Plants*; The American Chemical Society: Washington, DC, 1993.
18. Hostettmann, K.; Chinyanganya, F.; Maillard, M.; Wolfender, J.-L. *Chemistry, Biological and Pharmacological Properties of African Medicinal Plants*; University of Zimbabwe Publications: Mount Pleasant, 1996.
19. Allen, J. R.; Harris, C. R.; Danishefsky, S. J. *J. Am. Chem. Soc.* **2001**, *123*, 1890–1897.
20. Musselli, C.; Livingston, P. O.; Ragupathi, G. *J. Cancer Res. Clin. Oncol.* **2001**, *127*, R20–R26.
21. Krug, L. M. *Semin. Oncol.* **2004**, *31*, 112–116.
22. Jacobsen, N.; Fairbrother, W.; Kensil, C.; Lim, A.; Wheeler, D. A.; Powell, M. F. *Carbohydr. Res.* **1996**, *280*, 1–14.
23. Reynolds, W. F.; McLean, S.; Tay, L.-L.; Yu, M.; Enriquez, R. G.; Eastwick, D. M.; Pascoe, K. O. *Magn. Reson. Chem.* **1997**, *35*, 455–462.
24. Perlin, A. S.; Casu, B. *Tetrahedron Lett.* **1969**, 2921–2924.
25. Günther, H. *NMR Spectroscopy*, 2nd ed.; Wiley: New York, 1995. Chapter 2 and 5.
26. Cohen, A. D.; Sheppard, N.; Turner, J. J. *Proc. R. Soc. Lond., A* **1958**, 118–119.
27. Altona, C.; Haasnoot, C. A. G. *Org. Magn. Reson.* **1980**, *13*, 417–429.
28. Eliel, E. L.; Gianni, M. H.; Williams, T. H.; Stothers, J. B. *Tetrahedron Lett.* **1962**, 741–747.
29. Bang, S. C.; Lee, J. H.; Song, G. Y.; Kim, D. H.; Yoon, M. Y.; Ahn, B. Z. *Chem. Pharm. Bull.* **2005**, *53*, 1451–1454.
30. Jung, H.; Lee, C. O.; Lee, K. T.; Choi, J.; Park, H. J. *Biol. Pharm. Bull.* **2004**, *27*, 744–747.
31. Einbond, L. S.; Tao, S.; Wu, H.; Friedman, R. M.; Wang, X.; Ramirez, A.; Kronenberg, F.; Weinstein, I. B. *Int. J. Cancer* **2007**, *121*, 2073–2083.
32. Delaglio, F.; Grzesiek, S.; Vuister, G. W.; Zhu, G.; Pfeiffer, J.; Bax, A. *J. Biomol. NMR* **1995**, *6*, 277–293.
33. Davis, D. G.; Bax, A. *J. Am. Chem. Soc.* **1985**, *107*, 2820–2821.
34. Bothner-By, A.; Stephens, R. L.; Lee, J.-M.; Warren, C. D.; Jeanloz, R. W. *J. Am. Chem. Soc.* **1984**, *106*, 811–813.
35. Shaka, A. J.; Lee, C. J.; Pines, A. *J. Magn. Reson.* **1988**, *77*, 274–293.